



Reaction of titanium with carbon in a laser heated diamond anvil cell and reevaluation of a proposed pressure-induced structural phase transition of TiC

Björn Winkler^{a,*}, Erick A. Juarez-Arellano^a, Alexandra Friedrich^a, Lkhamsuren Bayarjargal^a, Jinyuan Yan^b, Simon Martin Clark^b

^a Institut für Geowissenschaften, Goethe-Universität Frankfurt, Altenhöferallee 1, 60438 Frankfurt a.M., Germany

^b Advanced Light Source, Lawrence Berkeley National Laboratory, MS6R2100, 1 Cyclotron Road, Berkeley, CA 94720-8226, USA

ARTICLE INFO

Article history:

Received 25 September 2008

Received in revised form 3 November 2008

Accepted 6 November 2008

Available online 14 November 2008

Keywords:

Laser heated diamond anvil cell

Titanium carbide

Phase transition

Density functional theory

ABSTRACT

The formation of cubic TiC_x from the elements was studied in a laser-heated diamond anvil cell at pressures up to 26 GPa. Annealed samples at these pressures show no splitting of the cubic (1 1 1) or (2 2 2) reflection. This is in contrast to an earlier study, in which a splitting of the (1 1 1) reflection was observed above 18 GPa. The recovered sample had a lattice parameter of 4.3238(6) Å, which implies that the synthesis gave fully stoichiometric TiC. Density functional theory-based model calculations were used to study the dependence of the total energy of a rhombohedral distortion. In these model calculations the total energy was minimal for the undistorted (cubic) lattice. Therefore, the results obtained here imply that at least for titanium carbides with a high carbon content no pressure-induced structural phase transition up to at least 26 GPa occurs. The appearance of a trigonal TiC_x polymorph during the synthesis is discussed in terms of its relative stability with respect to the cubic phase.

© 2008 Elsevier B.V. All rights reserved.

1. Introduction

The 'interstitial' carbides of group IV and group V elements are refractory, have high hardness and strength and often a high thermal and electrical conductivity. This makes them interesting candidate materials for applications such as coatings and diffusion barriers. Hence, their structure–property relations have been studied extensively, both experimentally and theoretically [1].

A typical representative of this group of compounds is TiC. Cubic δ-TiC crystallises in the NaCl-structure type, with space group Fm $\bar{3}$ m, and a lattice parameter of $a = 4.327(4)$ Å at ambient conditions. As with most carbides, the structure can accommodate a large concentration of defects on the 'interstitial' carbon positions, leading to substoichiometric TiC_x, with $1 > x > 0.5$. Lattice parameters and physical properties depend on the defect concentration. For example, the lattice parameter for a highly carbon deficient TiC_{0.5} = 4.30 Å [1].

Possible ordering schemes of the defects have been discussed controversially in the literature [2–5]. Regrettably, the nomenclature has been inconsistent, as phases with different crystal structures have been given the same designation in the case of δ'.

For low carbon concentrations (up to TiC_{0.71}), a cubic phase with space group symmetry Fd3m and twice the lattice parameter of the δ-phase has been reported [5] to be the stable phase at high temperatures above $T \approx 1050$ K. An ordered rhombohedral structure δ''-phase has been suggested to be stable at lower temperatures [6]. A trigonal structure with space group P31 or P3₁21 has been discussed by [3] and [2], respectively. These two space groups have the same reflection conditions. In a recent in situ neutron scattering study by Winkler et al. [7] only the cubic δ-phase was observed.

The synthesis of TiC at ambient pressure has been studied with various methods (see summary in Winkler et al. [7]) and the physical properties of TiC at ambient pressure have been extensively documented [1]. In contrast to these numerous studies at low and high temperatures, little is known about the pressure-dependence of structure–property relations. An initial study of the high pressure behaviour of TiC has been presented by Dubrovinskaia et al. [8]. In that study, a cubic to rhombohedral phase transition was found to occur at around 18 GPa. This was deduced from the observation of a splitting of the cubic (1 1 1) reflection. At 1 bar, the (1 1 1)-reflection had a FWHM of about 0.03 Å, while the reflection broadens to > 0.1 Å at 38 GPa. CsI was employed as a pressure-transmitting medium up to 18 GPa, while no pressure-transmitting medium was used at higher pressures. Diffractograms were collected with an in-house CCD camera mounted on a rotating anode generator. DFT model calculations, based on the FPLMTO method,

* Corresponding author.

E-mail address: B.Winkler@kristall.uni-frankfurt.de (B. Winkler).

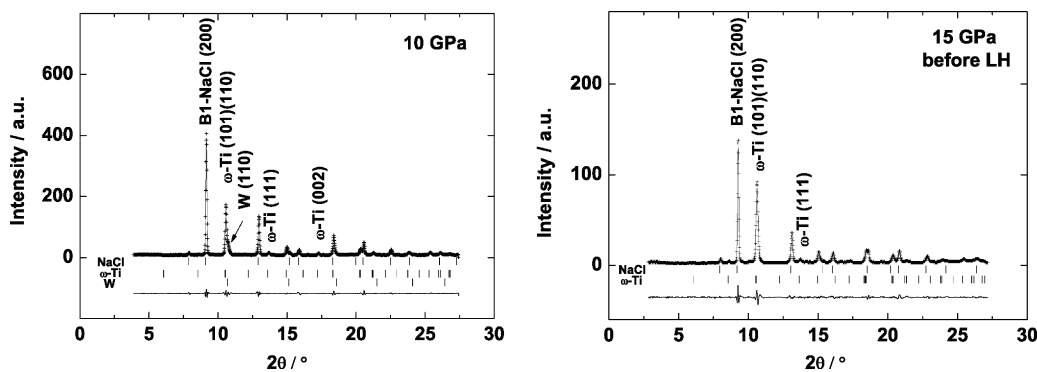


Fig. 1. Diffraction patterns before laser heating at 10 GPa (left) and 15 GPa (right). Only the starting materials can be detected, but the titanium has already transformed into the ω -polymorph.

were presented by Dubrovinskaia et al. [8] to support their findings, as these calculations showed a lowering of the total energy by a rhombohedral distortion on compression.

The exploratory study by Dubrovinskaia et al. [8] raised a number of questions, such as the pressure-dependence of the structural distortion. In the framework of a systematic study of the formation of transition metal carbides from the elements in laser heated diamond anvil cells, we therefore, studied the structure of TiC at high pressures in order to provide experimental constraints on the pressure-induced behaviour of this important transition metal carbide.

2. Experimental details

High pressure experiments were performed at the Advanced Light Source, ALS (Berkeley), on beam line 12.2.2 using 30 keV radiation. Double-sided laser heating was performed with fibre lasers. The experimental set-up is described in detail in Caldwell et al. [9].

We employed Boehler–Almax diamond anvil cells [10] with conical anvils, 0.35 mm culets and an effective aperture of $\approx 60^\circ$. We used tungsten gaskets, preindented to 42 μm . Gasket holes with a diameter of $\approx 120 \mu\text{m}$ were drilled by a home-built laser lathe. We used NaCl as a pressure medium and for thermal insulation. Titanium foil (Alpha Aesar, purity 99.99%) with a thickness of 25 μm and graphite, which has been characterised earlier [7] served as starting materials. Rubies were loaded to allow pressure determination by the ruby fluorescence method.

Due to the strong absorption of the laser radiation by the opaque samples, only moderate laser power ($< 20 \text{ W}$) was required to achieve bright hot spots indicating temperatures around 2000 K. However, due to technical problems with the temperature determination, only approximate temperatures to within 300 K could be determined. As the current study was aimed to observe reactions and characterise the products, this short-coming had no consequences in the present context.

Diffraction patterns were acquired with a MAR345 image plate detector. Counting times varied between 120 and 3600 s. Most data collection was done with a $10 \times 10 \mu\text{m}^2$ beam spot. The laser spots had a diameter of about 15–30 μm . Data analysis was performed with DatLab [11], Fit2D [12], GSAS [13] and Fullprof [14].

Pressures were determined with an off-line spectrometer using the ruby fluorescence method [15] and from the known equation of state for NaCl [16] during the diffraction measurements. The two pressures determined independently from each other agreed typically within 1 GPa.

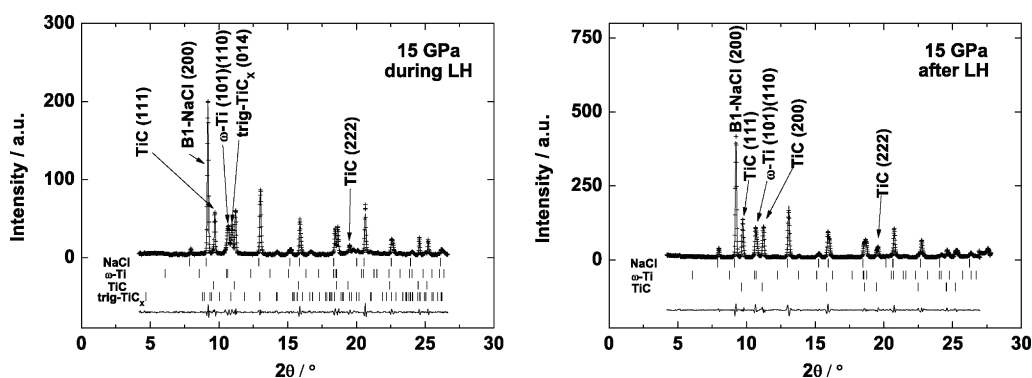


Fig. 2. Diffraction patterns during laser heating at 15 GPa (left) and after laser heating at the same pressure (right).

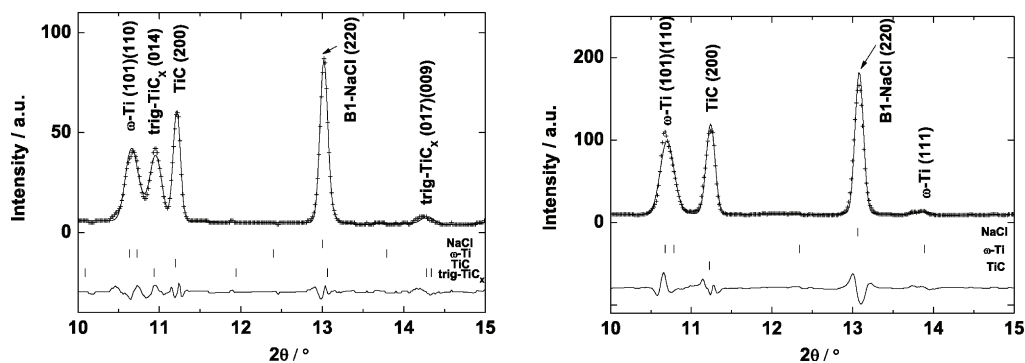


Fig. 3. Enlargement of the diffraction patterns during laser heating at 15 GPa (left) and after laser heating at the same pressure (right). During laser heating, the presence of a trigonal structure with lattice parameters of $a_{\text{hex}} = 3.074 \text{ \AA}$ and $c_{\text{hex}} = 14.877 \text{ \AA}$ could be deduced from several non-overlapping reflections.

Table 1
Phases and their lattice parameters identified in the diffraction patterns during the various runs.

P (GPa)	LH	Phase	S.G.	<i>a</i> (Å)	<i>c</i> (Å)	<i>V</i> (Å ³)
10	–	B1 NaCl	<i>Fm</i> $\bar{3}$ <i>m</i>	5.1764(2)	–	138.71(1)
		ω -Ti	<i>P</i> $\frac{O_3}{m}$ <i>mc</i>	4.4761(2)	2.7483(2)	47.686(5)
		W	<i>Im</i> $\bar{3}$ <i>m</i>	3.1214(3)	–	30.412(5)
15	Before	B1 NaCl	<i>Fm</i> $\bar{3}$ <i>m</i>	5.1126(3)	–	133.64(2)
		ω -Ti	<i>P</i> $\frac{O_3}{m}$ <i>mc</i>	4.4495(4)	2.7454(3)	47.072(8)
15	During	B1 NaCl	<i>Fm</i> $\bar{3}$ <i>m</i>	5.1547(2)	–	136.966(7)
		ω -Ti	<i>P</i> $\frac{O_3}{m}$ <i>mc</i>	4.4134(7)	2.7399(4)	46.220(1)
		TiC	<i>Fm</i> $\bar{3}$ <i>m</i>	4.2293(1)	–	75.650(3)
		trig-TiC _x	<i>P</i> 3121	3.0736(4)	14.877(3)	121.86(3)
15	After	B1 NaCl	<i>Fm</i> $\bar{3}$ <i>m</i>	5.1297(2)	–	134.985(8)
		ω -Ti	<i>P</i> $\frac{O_3}{m}$ <i>mc</i>	4.4335(3)	2.6743(9)	45.52(2)
		TiC	<i>Fm</i> $\bar{3}$ <i>m</i>	4.2195(2)	–	75.126(5)
25	Before	B1 NaCl	<i>Fm</i> $\bar{3}$ <i>m</i>	4.9657(5)	–	122.45(2)
		ω -Ti	<i>P</i> $\frac{O_3}{m}$ <i>mc</i>	4.4043(6)	2.68(2)	45.1(3)
		W	<i>Im</i> $\bar{3}$ <i>m</i>	3.1051(3)	–	29.939(5)
25	After	B1 NaCl	<i>Fm</i> $\bar{3}$ <i>m</i>	4.8996(5)	–	117.62(1)
		B2 NaCl	<i>Pm</i> $\bar{3}$ <i>m</i>	3.0410(3)	–	28.123(5)
		W	<i>Im</i> $\bar{3}$ <i>m</i>	3.0925(6)	–	29.58(1)
		TiC	<i>Fm</i> $\bar{3}$ <i>m</i>	4.1787(4)	–	72.97(1)
		Ruby	<i>R</i> $\bar{3}$ <i>c</i>	4.531(1)	12.147(4)	215.9(1)
Recovered	–	B1 NaCl	<i>Fm</i> $\bar{3}$ <i>m</i>	5.6321(2)	–	178.65(1)
		ω -Ti	<i>P</i> $\frac{O_3}{m}$ <i>mc</i>	4.7027(2)	2.8426(3)	54.442(7)
		TiC	<i>Fm</i> $\bar{3}$ <i>m</i>	4.3116(2)	–	80.154(5)
		W	<i>Im</i> $\bar{3}$ <i>m</i>	3.1495(6)	–	31.24(1)

LH, laser heating; S.G., space group.

3. Results

The first set of data were collected at 10 GPa. The pressure determined by ruby fluorescence was 9.9(2) GPa, while pressure from the equation of state of NaCl was 10.6(2) GPa. At that pressure, the titanium had transformed from the hcp α -structure to the ω -polymorph, with $a_{\omega}(\text{Ti}, 10 \text{ GPa}) = 4.4761(2) \text{ \AA}$ and $c_{\omega}(\text{Ti}, 10 \text{ GPa}) = 2.7483(2) \text{ \AA}$. The diffractogram obtained before any heating (Fig. 1) could be fully indexed by an assignment of peaks to either Ti, W (from the gasket), or NaCl (used in the thermal insulation). Due to its comparatively low scattering cross-section, carbon could not be detected. At 15 GPa, the diffractogram only shows reflections of NaCl and ω -Ti (Fig. 1) and the values for the lattice parameters of titanium decreased to $a_{\omega}(\text{Ti}, 15 \text{ GPa}) = 4.4495(4) \text{ \AA}$ and $c_{\omega}(\text{Ti}, 15 \text{ GPa}) = 2.2454(3) \text{ \AA}$. These values are in very good agreement with those listed by Errandonea et al. [17], who studied the influence of the pressure medium on the transition pressure of titanium by diffraction.

Laser heating with moderate laser power (around 10–15 W per laser) led to temperatures of about 1600–2200 K in the sample. Experience shows that the optical emission of samples which react

on laser heating is very variable and a more reliable temperature determination was not possible. These (P,T)-conditions led to the formation of cubic TiC and, during some heating experiments, also of trigonal TiC_x (Figs. 2 and 3). Trigonal TiC_x was identified from several non-overlapping reflections (Fig. 3) but was only observed during a few measurements at 15 GPa. We did not detect any trace of the trigonal phase at higher pressures or in the recovered sample.

The lattice parameters of all phases identified at various run conditions are given in Table 1. Clearly, it is not possible from the data obtained here to determine the exact composition of the carbides at high (P,T)-conditions, as sub-stoichiometry will have the same effect on the lattice parameter as pressure. Non-stoichiometry at ambient conditions leads to changes in the lattice parameter of less than 0.03 Å. This uncertainty, in conjunction with the few data points, prevents a reliable determination of an equation of state. However, as will be described below, the final product was stoichiometric or near-stoichiometric TiC and so the problem of non-stoichiometry may be non-existent at high (P,T)-conditions.

A cubic-to-rhombohedral phase transformation was suggested to occur for TiC at $\approx 18 \text{ GPa}$ [8]. In order to quantify the proposed splitting of the cubic (1 1 1) reflection with a higher resolution than

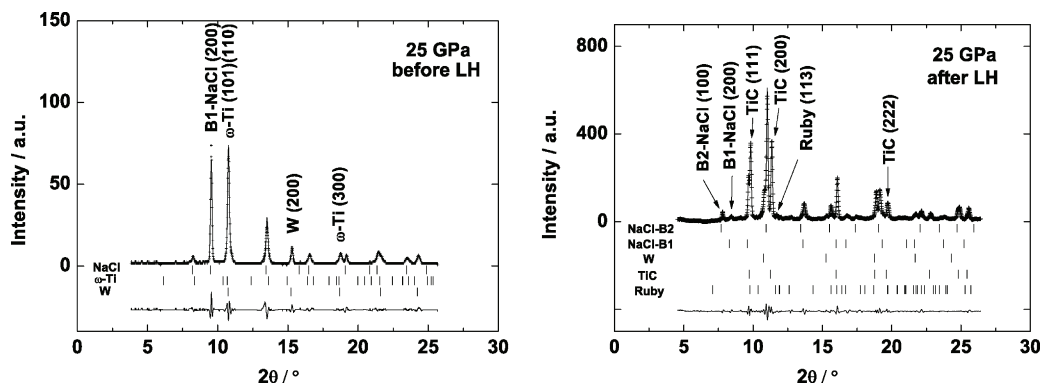


Fig. 4. Diffractograms recorded at 25 GPa before (left) and after (right) laser heating.

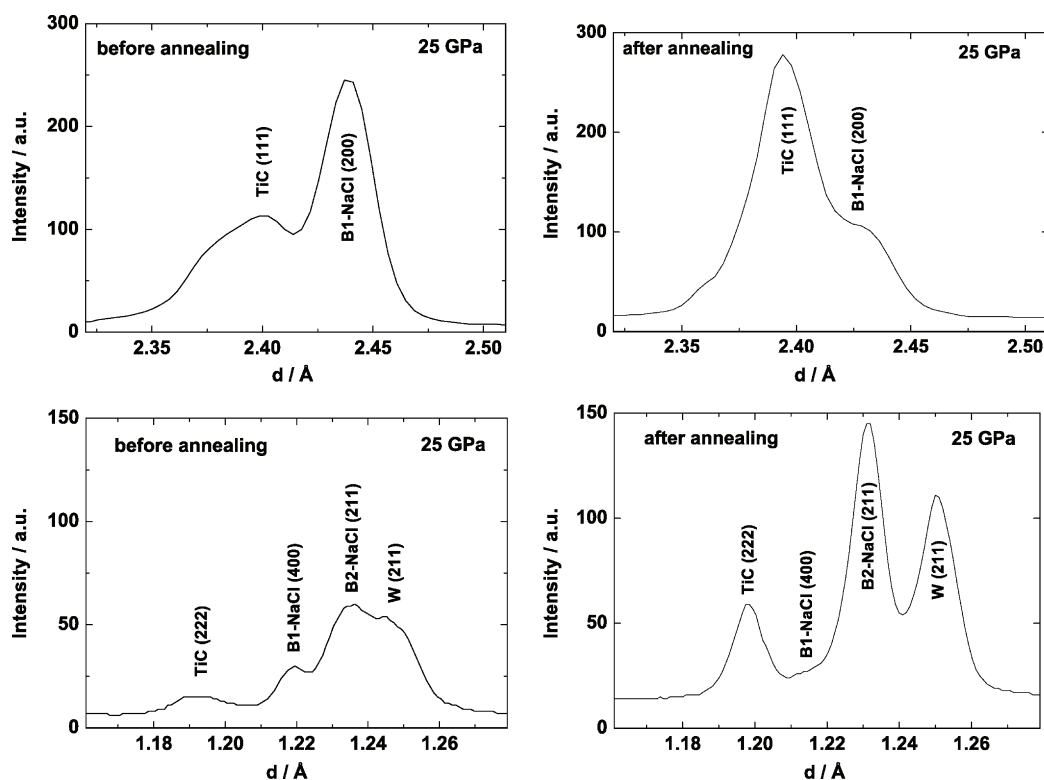


Fig. 5. Diffraction patterns before and after annealing the sample at 25 GPa. The top row shows the cubic (1 1 1) reflection of TiC, the lower row shows the cubic (2 2 2) reflection.

was available in the earlier study, we increased the pressure to 25 GPa and annealed the sample by scanning it from one side with low laser power. The results are shown in Fig. 4. Before laser heating, we observe NaCl in the B1 structure type, ω -Ti and tungsten from the gasket. After laser heating, we have NaCl both in the B1 and B2 structure type, cubic TiC and we also observe reflections belonging to the ruby crystal. At the laser heated spot there was no remaining titanium within the detection limit, which is estimated at a few vol%.

As is well known, annealing greatly reduces residual strain induced by deviations from hydrostaticity. This is also observed here. An enlargement of the regions around the cubic (1 1 1) and (2 2 2) reflections of TiC is shown before and after laser heating in Fig. 5. The FWHM of the (1 1 1) and (2 2 2) reflections after annealing were ≈ 0.03 Å, and hence no broadening was detectable. The (1 1 1)

slightly overlaps with B1-type NaCl-(2 0 0), but the non-overlapping (2 2 2) also clearly shows no splitting.

No further phases were observed on laser-heating at 25 GPa, either on regions of the sample which had been reacted before at lower pressures or on regions in which there was still titanium present. Hence, we conclude that the stable carbide phase at these conditions is TiC and that the stability field of TiC extends to at least (2000 K, 25 GPa).

The diffraction pattern of the recovered sample (i.e. sample in the gasket measured outside the DAC) is shown in Fig. 6. The lattice parameter of the recovered TiC sample is $a(\text{TiC}, 1 \text{ bar}) = 4.3238(6)$ Å. The precision of this result can be estimated by a comparison of the lattice parameter of NaCl in the recovered sample. We determined $a(\text{NaCl}, 1 \text{ bar}) = 5.6352(7)$ Å, while literature values for ambient conditions range from 5.639 to 5.644 Å [18]. Fully stoichiometric TiC has a lattice parameter of ≈ 4.327 Å and a carbon deficiency causes the lattice parameter to shrink down to 4.30 Å for $\text{TiC}_{0.5}$. Hence, the sample synthesised at high (P,T) conditions seems to be fully stoichiometric.

4. DFT model

The experiments discussed above indicated that there was no rhombohedral distortion in our experiments, while in Dubrovinskaia et al. [8] DFT-FPLMTO models gave a small rhombohedral distortion at a 5% compression. Density functional theory calculations have extensively been used to model structure–property relations of carbides and hence, we thought it worthwhile to re-determine the energy gain through the rhombohedral distortion.

We have shown in an earlier paper [7] that a DFT-based model using the generalised gradient approximation, a plane wave basis set and ultrasoft pseudopotentials satisfactorily reproduced structures and properties of titanium and TiC. We therefore continued these calculations here. We used commercial and academic versions of CASTEP [19]. Concurrent geometry optimisations of unit

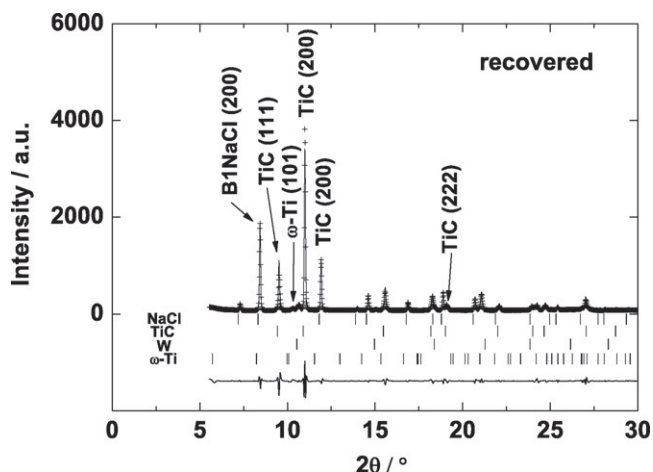


Fig. 6. Diffraction pattern of the recovered sample.

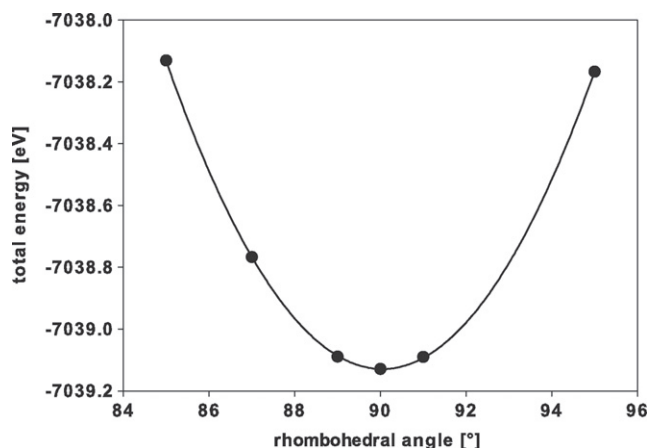


Fig. 7. Total energy of TiC as a function of an imposed rhombohedral angle at constant volume $V = 0.93V_0$, corresponding to 20 GPa. Clearly, the energy minimum corresponds to the cubic structure.

cell and internal coordinates were performed so that forces were converged to 0.005 eV/Å and stress residual to 0.005 GPa.

The theoretical lattice parameter $a(\text{TiC, theo}) = 4.333 \text{ \AA}$ shows the expected good agreement with the experimental value obtained here ($a(\text{TiC, exp, 1 bar}) = 4.324 \text{ \AA}$). Elastic properties have been obtained from stress–strain calculations, and the corresponding theoretical values are: bulk modulus $B(\text{TiC, theo}) = 227(1) \text{ GPa}$, Voigt shear stiffness $\mu_{\text{Voigt}}(\text{TiC, theo}) = 168.5 \text{ GPa}$, Reuss shear stiffness $\mu_{\text{Reuss}}(\text{TiC, theo}) = 168.2 \text{ GPa}$, Young's modulus $E(\text{TiC, theo}) = 419.9 \text{ GPa}$, and Poisson ratio $\sigma(\text{TiC, theo}) = 0.19$. All these values are in the expected good agreement with the corresponding experimental data [20], which depend slightly on composition: bulk modulus $B(\text{TiC, exp}) = 232\text{--}253 \text{ GPa}$, shear stiffness $\mu(\text{TiC, exp}) = 164\text{--}190 \text{ GPa}$, Young's modulus $E(\text{TiC, exp}) = 436\text{--}462 \text{ GPa}$, and Poisson ratio $\sigma(\text{TiC, exp}) = 0.17\text{--}0.25$. This demonstrates again the reliability of the model calculations.

The energy as a function of an imposed rhombohedral angle at a $V/V_0 = 0.93$, corresponding to a pressure of 20 GPa, is shown in Fig. 7. Clearly, it has a minimum at an angle of 90° , i.e. according to our DFT calculations, and in agreement with our experiments, there is no transformation to a structure with lower symmetry.

We also studied the trigonal polymorph. It is generally not straightforward to model the stability of defect structures with DFT models such as those employed here, as these would require large supercell calculations and sophisticated models to study the short-range ordering behaviour of defects. However, as was the case in our earlier model calculations, where we simulated the incorporation of carbon into titanium, models neglecting short-range ordering can provide semiquantitative information of the role of defects.

We first described cubic TiC in a trigonal coordinate system. The corresponding structure has space group symmetry $R\bar{3}m$ with full occupation of the carbon sites. After the geometry optimisation, this structure has lattice parameters of $a_{\text{trig}}(\text{Ti}_6\text{C}_6) = 3.086 \text{ \AA}$ and $c_{\text{trig}}(\text{Ti}_6\text{C}_6) = 15.118 \text{ \AA}$ and the maximal displacement of an atom from its position in the NaCl-type structure was 0.0008 \AA . Hence, the trigonal structure is indistinguishable from the cubic structure and a fully occupied trigonal polymorph does not exist. However, the lattice parameters of the trigonal structure in which all carbon sites are occupied are already very close to the experimentally observed values (Table 1), and this implies, that only small structural changes are required. Geometry optimisation calculations after partially removing carbon atoms from the trigonal structure showed the expected behaviour, namely that the a -lattice parameter is only slightly dependent on the carbon content, while the c -lattice parameter shrinks significantly, e.g. to 14.489 \AA for Ti_6C_3 .

Neglecting the influence of pressure and temperature, the carbon deficient structures are always stable with respect to a mechanical mixture of the elements. Hence, they can appear at least as metastable phases. We can calculate reaction energies, for example for the reaction



In this reaction, the cubic phase is more stable by 63 kJ/mol of TiC, and hence, in a carbon saturated environment, we expect cubic TiC to be the product. This is consistent with the observations we made in our experiments. On the other hand, for the reaction



we predict that the trigonal phase is more stable by 25 kJ/mol of Ti_2C , so that in a carbon undersaturated environment, the trigonal phase may become the dominant product.

Due to the approximations made, these calculations are only indicative, but we believe that the DFT model captures the essence of the reaction and the structures involved, namely the existence of a trigonal defect structure, which c -lattice parameter strongly depends on the carbon concentration and which has an energy not too different from the cubic phase. All results from the model calculations are fully consistent with the experimental observations.

The existence of a trigonal phase required additional high pressure calculations, as, due to different symmetry constraints, this structure could have a different distortion mechanism on pressure increase than a structure which is constrained to have cubic symmetry. However, after geometry optimisations at 40 GPa, the relaxed trigonal structure with full occupation of all carbon positions could again be transformed without distortion into a cubic structure and hence, also at 40 GPa, no stoichiometric trigonal structure exists.

5. Summary

The results obtained here from experiments and model calculations indicate that TiC does not undergo a structural phase transition up to 25 GPa, the highest pressure studied here. Our results also imply that, while a trigonal polymorph can be synthesised at high pressures, it is, in the presence of excess carbon, always less stable than stoichiometric cubic carbide.

Acknowledgements

This research was supported by Deutsche Forschungsgemeinschaft (Project WI-1232), in the framework of the DFG-SPP 1236. AF thanks the CNV-Foundation for financial support. The Advanced Light Source is supported by the Director, Office of Science, Office of Basic Energy Sciences, of the U.S. Department of Energy under Contract No. DE-AC02-05CH11231. This research was partially supported by COMPRES, the Consortium for Materials Properties Research in Earth Sciences under NSF Cooperative Agreement EAR 06-49658.

References

- [1] H.O. Pierson, Handbook of Refractory Carbides, Noyes Publication, Estwood, New Jersey, USA, 1996.
- [2] B.V. Khaenko, V.V. Kukul, Kristallografiya 34 (1989) 1513–1517.
- [3] V.V. Kukul, B.V. Khaenko, O.A. Gnitetskii, Kristallografiya 40 (1995) 75–78.
- [4] A.I. Gusev, Physics–Uspekhi 43 (2000) 1–37.
- [5] M.Y. Tashmetov, V.T. Em, C.H. Lee, H.S. Shim, Y.N. Choi, J.S. Lee, Physica B 311 (2002) 318–325.
- [6] V.T. Em, M.Y. Tashmetov, Physica Status Solidi (b) 198 (1996) 571–575.
- [7] B. Winkler, D.J. Wilson, S.C. Vogel, D.W. Brown, T.A. Sisneros, V. Milman, Journal of Alloys and Compounds 441 (2007) 374–380.
- [8] N.A. Dubrovinskaia, L.S. Dubrovinsky, S.K. Saxena, R. Ahuja, B. Johansson, Journal of Alloys and Compounds 289 (1999) 24–27.

- [9] W. Caldwell, M. Kunz, R. Celestre, E.E. Domning, M.J. Walter, D. Walker, J. Glossinger, A.A. MacDowell, H.A. Padmore, R. Jeanloz, S.M. Clark, *Nuclear Instruments and Methods in Physics Research A* 582 (2007) 221–225.
- [10] R. Boehler, *Review of Scientific Instruments* 77 (2006) 115103.
- [11] K. Syassen, *Datlab. Version 1.37d*, MPI/FKF, Stuttgart, Germany, 2005.
- [12] A.P. Hammersley, S.O. Svensson, M. Hanfland, A.N. Fitch, D. Hauserman, *High Pressure Research* 14 (1996) 235–248.
- [13] A. Larson, R. Von Dreele, *General Structure Analysis System (GSAS)*, Los Alamos National Laboratory Report LAUR (2004) 86–748.
- [14] J. Rodriguez-Carvajal, *Physica B* 192 (1993) 55–69.
- [15] H. Mao, P. Bell, J. Shaner, D. Steinberg, *Journal of Applied Physics* 49 (1978) 3276–3283.
- [16] M. Chall, B. Winkler, P. Blaha, K. Schwarz, *Journal of Physical Chemistry B* 104 (2000) 1191–1197.
- [17] D. Errandonea, Y. Meng, M. Somyazulu, D. Häusermann, *Physica B* 355 (2005) 116–125.
- [18] ICSD, *Inorganic Crystal Structure Database*, National Institute of Standards and Technology, Gaithersburg (2007).
- [19] S.J. Clark, M.D. Segall, C.J. Pickard, P.J. Hasnip, M.J. Probert, K. Refson, M.C. Payne, *Zeitschrift für Kristallographie* 220 (2005) 567–570.
- [20] S.P. Dodd, M. Cankurtaran, B. James, *Journal of Material Science* 38 (2003) 1107–1115.